THE ASTROPHYSICAL JOURNAL, 507:229–240, 1998 November 1

STAR FORMATION AND CHEMICAL EVOLUTION IN THE MILKY WAY: COSMOLOGICAL IMPLICATIONS

NIKOS PRANTZOS[1] AND JOSEPH SILK[1,2]
Received 1998 March 31; accepted 1998 June 5

ABSTRACT

We propose an expression for the star formation rate in spiral galaxies and a model of chemical evolution with a minimal number of adjustable parameters. Our model accounts for most of the relevant data in the Milky Way. By adopting our Galaxy as a prototype, we are able to derive cosmological implications for the comoving star formation rate, gas amount, gaseous abundances, and supernova rates as a function of redshift.

Subject headings: galaxies: evolution — Galaxy: evolution — solar neighborhood

1. INTRODUCTION

The star formation rate is crucial for understanding galaxy formation and evolution. Our observations of the most distant galaxies primarily probe star formation rates and the consequences thereof. Yet prescriptions for star formation leave much to be desired. Numerical simulations commonly assert that star formation is a simple function of local density. Clearly, there is more than this to star formation. Another approach models the star formation rate in nearby galaxies with a single parameter, the characteristic star formation timescale, and builds up a luminosity function of appropriate Hubble types that can be tracked back in time. This approach ignores the fact that tidal interactions and mergers become increasingly frequent beyond redshift unity, and that such environmental effects may stimulate star formation in a more complex fashion, involving additional parameters. It is therefore not particularly surprising that neither ab initio simulations of galaxy formation (Lacey et al. 1997) nor studies of backward evolution (Bouwens, Cayon, & Silk 1997; Madau, Pozzetti, & Dickinson 1997) have succeeded in adequately modeling the observed star formation rate per unit volume, especially between redshifts 0 and 3.

Any reliable prescription for star formation must ultimately depend on local studies, especially of the Milky Way Galaxy, and in particular the solar vicinity. Observations of the gas and star densities, chemical abundances in gas and stars as functions of Galactocentric radius and age, and the distribution of stellar metallicities and abundance gradients are all intimately associated with the rate of star formation, both today and in past epochs. In this paper, we refine a prescription for star formation from our earlier work that includes all of these data. We then apply the model at cosmological distances, in order to investigate the cosmic star formation rate, elemental abundances, and gas fraction as a function of redshift for Milky Way–type galaxies. Comparisons with recent observations of these quantities at high redshift show whether or not the evolution of Milky Way spirals is representative of the cosmic chemical evolution.

The plan of the paper is as follows. In § 2 we present the chemical evolution model and its main ingredients. In § 3 we apply our model to the Milky Way Galaxy and compare the results to the various observational constraints. In § 4 we translate our results to a cosmological framework and compare them to various quantities observed as a function of redshift. The results of this comparison are summarized in § 5.

2. THE MODEL

Variations on a particularly simple but compelling model for the global Galactic star formation rate and chemical evolution in our Galaxy have been presented previously (e.g., Wang & Silk 1994; Prantzos & Aubert 1995, hereafter PA95). Here we summarize the basic features of our preferred model and present the updated input physics.

We solve numerically the classical set of equations of galactic chemical evolution (Tinsley 1980; Pagel 1997), without invoking the instantaneous recycling approximation (IRA). Instantaneous mixing of the gas with the stellar ejecta is assumed, i.e., the gas is characterized by a unique composition at each point in time. The adopted stellar lifetimes are from Schaller et al. (1992) for metallicity $Z = Z_{\odot}$; note that the metallicity dependence of the stellar lifetimes does not help to resolve the G-dwarf problem in the solar neighborhood (Bazan & Mathews 1992; Rocha-Pinto & Maciel 1997). We adopt the following prescriptions for the masses of the stellar remnants. Stars of mass $M < 9\ M_{\odot}$ become white dwarfs with mass $M_R(M) = 0.1\ M + 0.45$ (Iben & Tutukov 1984; masses are expressed in $M_{\odot}$). Stars of $M > 9\ M_{\odot}$ explode as Fe core–collapse supernovae, leaving behind a neutron star of mass $M_R = 1.5\ M_{\odot}$ (as suggested by observations of neutron stars in binary systems); the heaviest of these stars may form black holes, but the mass limit for black hole formation is not known at present and cannot be inferred from theoretical or observational arguments (e.g., Prantzos 1994; Bethe & Brown 1995; Timmes, Woosley, & Weaver 1996), despite occasional claims to the contrary. Fortunately, because of the steeply decreasing stellar initial mass function (IMF) in the range of massive stars, the mass limit for stellar black hole formation does not significantly affect the results of chemical evolution, at least in so far as this limit is above $\sim 30\ M_{\odot}$.

The yields of massive stars adopted in this work are those of Woosley & Weaver (1995, hereafter WW95) for metallicity $Z = Z_{\odot}$. Note that in some cases their yields differ considerably from the corresponding yields of the other major recent work in this area (Thielemann et al. 1996).

[1] Institut d'Astrophysique de Paris, CNRS, 98 bis Boulevard Arago, 75014 Paris, France.
[2] Departments of Astronomy and Physics, University of California at Berkeley, Berkeley, CA 94720-3411.

These differences are due to the different physical inputs utilized by the two groups, principally the criterion for convection, the nuclear reaction rates, and the determination of the mass cut (see Prantzos 1998b for a review of the role of massive star yields in chemical evolution). The most significant difference concerns the yield of Fe; WW95 find that the Fe yield increases with stellar mass, while Thielemann et al. (1996) obtain a value that is approximately constant at $\sim 0.07\ M_\odot$.

There are equally important uncertainties in the yields of $M < 9\ M_\odot$ stars, due to, for example, the treatment of mass loss and envelope convection, especially during the final evolution on the asymptotic giant branch (AGB; see Charbonnel 1998 for a recent review). Here we have adopted the yields of Marigo, Bresan, & Chiosi (1996) in the 1–4 $M_\odot$ range and the yields of Renzini & Voli (1981) in the 4–9 $M_\odot$ range (see their Table 4d with hot bottom burning); despite the different physical inputs, the two sets of yields merge rather smoothly in the intermediate-mass regime ($\sim 4\ M_\odot$). In any case, the uncertainties in these yields play a very limited role in the context of the present work.

The adopted stellar IMF is from the work of Kroupa, Tout, & Gilmore (1993), where the complex interdependence of several factors (such as stellar binarity, age, and metallicity, as well as the mass-luminosity and color-magnitude relationship) is explicitly taken into account in the derivation of the IMF, described by a three-slope power law, $\Phi(M) \propto M^{-(1+x)}$, in the interval 0.1–100 $M_\odot$. In the high-mass regime, the IMF has a relatively steep slope of $x = 1.7$, while it flattens in the low-mass range ($x = 0.3$ for $M < 0.5\ M_\odot$), as indicated by recent observations with the *Hubble Space Telescope* (*HST*) (e.g., Gould, Bahcall, & Flynn 1997). The adopted IMF is normalized to $\int_{0.1}^{100} M\Phi(M)dM = 1$. The corresponding return mass fraction (i.e., the expression $R = \int_1^{100} (M - M_R)\Phi(M)dM$ is found to be $R \sim 0.32$.

The adopted star formation rate (SFR) Ψ is locally a Schmidt-type law, $\Psi \propto \Sigma_G^{1.5}$, where Σ_G is the local gas surface density (Kennicutt 1989). Across the Galactic disk, the star formation rate is modified by a radius-dependent factor, $\Psi(R) \propto \Sigma_G(R)/R$, motivated by the theory of star formation induced by spiral density waves in galactic disks (Wyse & Silk 1989); such a radial dependence allows us to account for the observed gradients of the gas, SFR, and chemical abundance profiles in the Milky Way (e.g., PA95 and § 3.2), as well as the observed photometric profiles of spiral galaxies (Boissier & Prantzos 1998).

Once the SFR and IMF are fixed, and the lower mass limit $M_{\rm SN\,II}$ for the formation of Fe core–collapse supernovae is determined, the corresponding rate of supernova explosions can be calculated as SN $\mathrm{II}(t) = \Psi(t) \int_{M_{\rm SN\,II}}^{100\,M_\odot} \Phi(M)dM$; we adopt here $M_{\rm SN\,II} = 9\ M_\odot$ (in fact, the most massive of these stars, as well as some of those in close binary systems, will suffer extensive mass losses prior to the explosion and appear as SNe Ib/c, but we retain the designation of SN II for all Fe core–collapse events). On the other hand, a supplementary source of Fe peak nuclei is introduced in the form of Type Ia supernovae (SNe Ia), presumably white dwarfs in binary systems accreting material from their companion stars (see Nomoto, Iwamoto, & Kishimoto 1997 for a recent review of SNe Ia). The relative homogeneity of the observed SN Ia light curves suggests that $\sim 0.7\ M_\odot$ of Fe is ejected (originally in the form of ^{56}Ni); this is also predicted by the most successful models of SNe Ia, involving carbon deflagration in a Chandrasekhar-mass white dwarf. We adopt here the yields of the W7 model from Thielemann, Nomoto, & Yokoi (1986). However, the evolution of the SN Ia rate in the Galaxy is difficult to predict from the theory of binary systems alone (see, e.g., Ruiz-Lapuente & Canal 1998 and references therein). We adopt here the prescription of Matteucci & Greggio (1986) for the death rates of secondaries in binary systems, introducing a time-delay parameter in order to reproduce the observed decline of O/Fe in the local disk (see § 3.1).

Finally, our model includes infall, i.e., the disk is assumed to be built up by accretion of gas with primordial composition. On purely phenomenological grounds, infall constitutes the most elegant and natural way of accounting for the G-dwarf problem in the solar neighborhood (e.g., Tinsley 1980; Pagel 1997), but infall is also supported by some chemodynamical models of the Milky Way (Samland, Hensler, & Theis 1997). The infall rate is locally adjusted to account for the observed G-dwarf metallicity distribution, but it is unconstrained in other regions of the disk (see § 3.2).

3. THE EVOLUTION OF THE MILKY WAY

The Milky Way is a heterogeneous system, with at least three components (halo, bulge, disk) having very different chemical, photometric, and kinematical properties. A reliable model for the evolution of the Milky Way that accounts for these properties does not exist at present. In particular, it is not clear how the various components are related, e.g., whether the evolution of the halo has significantly affected the bulge or the disk (and vice versa). Neither is it clear whether there has been significant interaction between the various parts of the disk through large-scale gas movements in the radial direction. Despite the development of various models, all these issues are still open.

For the purposes of this work, we adopt a very simple model for the chemical evolution of the Galactic disk and the bulge. We choose to ignore the Galactic halo, not only because its coupling to the disk is not understood, but also because its small present-day stellar mass suggests that halo star formation has never dominated the SFR of the Galaxy. In our model we are guided by phenomenology rather than theoretical principles, and we try to construct a model that reproduces the major observational constraints of the Milky Way with a minimum number of free parameters.

3.1. *The Solar Neighborhood*

In the solar neighborhood (defined as a cylinder of ~ 1 kpc radius at a distance $R_\odot = 8.5$ kpc from the Galactic center), the main observables relevant to chemical evolution are (see also PA95; Pagel 1997; and Fig. 1):

1. The current surface densities of gas and stars and the total amount of matter ($\Sigma_G \sim 10$, $\Sigma_* \sim 40$, and $\Sigma_T \sim 55\ M_\odot\ \mathrm{pc}^{-2}$, respectively; see Sackett 1997 and references therein for a recent review), leading to a current gas fraction of $\sigma_G \sim 20\%$ and a current star formation rate of 3–5 $M_\odot\ \mathrm{pc}^{-2}\ \mathrm{Gyr}^{-1}$ (e.g., Rana 1991 and references therein).

2. The abundances of various elements and isotopes at solar birth ($X_{i,\odot}$; meteoritic values from Anders & Grevesse 1989) and today ($X_{i,0}$). Note that measurements show $X_{i,0} < X_{i,\odot}$ (at least for CNO elements) both in the local interstellar medium (Cardelli & Federman 1997) and in nearby young stars in Orion (Cunha & Lambert 1994), sug-

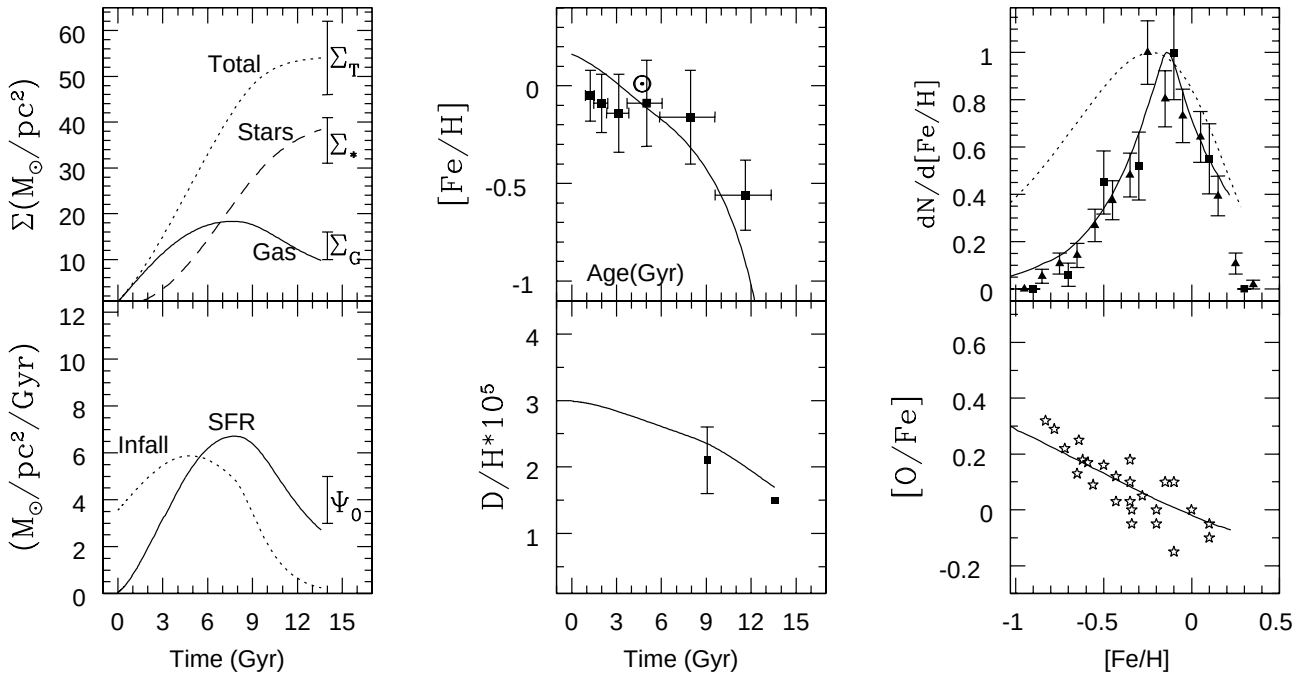

FIG. 1.—Main observational constraints on the chemical evolution of the solar neighborhood, compared to the results of the model presented in § 3.1 *Left top panel*: Local surface densities of gas (Σ_G), stars (Σ_*), and total amount of matter (Σ_T). Currently observed values are indicated on the right, between vertical error bars. The corresponding model results are indicated by solid, dashed, and dotted lines, respectively. *Left bottom panel*: Rates of infall (*dotted line*) and star formation (SFR, *solid line*); the latter is to be compared to the currently observed $\Psi_0 \sim 3$–$5\ M_\odot\ pc^{-2}\ Gyr^{-1}$ (vertical error bar on the right). *Middle top panel*: Age-metallicity relationship in the solar neighborhood (from Table 14 of Edvardsson et al. 1993). The data (for 182 F-type stars) are binned in groups of 0.2 in log (age), where the age is expressed in Gyr. Metallicities are for stars with Galactocentric distances evaluated to 8–9 kpc, i.e., appropriate to the solar neighborhood only and volume-corrected (see col. [6] in Table 14 of Edvardsson et al. 1993). The vertical error bars represent 1 σ dispersion in metallicity for each age group (see col. [6] in Table 15 of Edvardsson et al. 1993). The solid line shows the result of the model. *Middle bottom panel*: Evolution of deuterium. Data points for presolar D/H are from Geiss & Gloeckler (1998), and for the local ISM are from Linsky (1998). *Right top panel:* Metallicity distributions of G-type stars in the solar neighborhood. Data are from Rocha-Pinto & Maciel (1996) (*triangles*) and Wyse & Gilmore (1995) (*squares*). Solid line shows the model results; dotted line shows the results of a closed-box model, included for illustration purposes. *Right bottom panel*: O vs. Fe relationship in the local disk. Data are from Edvardsson et al. (1993). The observed decline of O/Fe is attributed to the delayed appearance of SN Ia, producing $\sim\frac{2}{3}$ of the solar Fe.

gesting that $X_\odot$ is perhaps not representative of the local ISM 4.5 Gyr ago. Some other arguments concerning various isotopic ratios (e.g., Wielen, Fuchs, & Dettbarn 1996; Clayton 1997) also point in this direction. If this turns out to be true, it would have major implications for chemical evolution studies; indeed, all models at present are required to reproduce solar elemental and isotopic abundances at the time of solar system formation.

3. The oxygen versus Fe (O-Fe) relationship, which exhibits a steady decline from O/Fe ~ constant ~ 3 times solar at [Fe/H] < -1 (i.e., during the halo phase) to O/Fe ~ solar at [Fe/H] ~ 0; this is usually attributed to the delayed (~1 Gyr) appearance of SNe Ia, producing $\sim\frac{2}{3}$ of the Galactic Fe, while $\sim\frac{1}{3}$ of the Fe and all of the O are produced by short-lived massive stars exploding as SN II. Note that the time delay of SN Ia activity (~1 Gyr) is dictated by our understanding of the halo formation timescale, and not by any understanding of the SN Ia frequency; despite the use of some "sophisticated" formulae (involving, e.g., the orbital period and mass ratio of the binary system), the SN Ia rate is essentially a free parameter of the models, unlike the SN II rate. In particular, it is not at all clear why the end of the halo phase (determined by large-scale dynamical processes in the Galaxy) coincides with the onset of the decline in the O/Fe ratio (dictated by dynamical processes in binary systems involving white dwarfs). This may be only a coincidence, and need not be the case in the inner or outer zones of the disk.

4. The age-metallicity relationship, traced by the Fe abundance of long-lived F-type stars. The data (Edvardsson et al. 1993 and Fig. 1) show a monotonic increase in the mean metallicity and a considerable dispersion at any age; the latter, if real, may result from imperfect mixing of the ISM, orbit diffusion of stars coming from Galactic regions with different metallicities (Wielen, Fuchs, & Dettbarn 1996), or both. Simple one-zone chemical evolution models always yield unique age-metallicity relationships and cannot reproduce the scatter without further assumptions and free parameters (see the recent studies by Pilyugin & Edmunds 1996 and van den Hoek & de Jong 1997 on inhomogeneous chemical evolution of the local disk). Note that a recent reanalysis of the Edvardsson et al. (1993) data (Ng & Bertelli 1997) concludes that the resulting age-metallicity relationship is somewhat different, i.e., that (1) stellar ages are slightly larger than derived in Edvardsson et al. (1993), and (2) only for the oldest stars is there a net trend of variation in metallicity with age.

5. The metallicity distribution of long-lived G-type stars (Fig. 1), which shows that very few disk stars were formed at [Fe/H] < -0.7 ($<\frac{1}{5}$ solar). This is the most important constraint, never satisfied in models of the local disk that form rapidly (such as homogeneous closed-box models or models that assume infall on short timescales). The alternative solution, namely that the disk started with an initial metallicity of [Fe/H] $= -0.7$ (corresponding to [O/H] ~ -0.4, or $\sim\frac{1}{3}$ solar) is rather implausible, since neither the Galactic

halo nor the bulge is massive enough to have polluted the disk to such an extent. Note that recent data sets (Wyse & Gilmore 1995; Rocha-Pinto & Maciel 1996) show a narrower metallicity distribution than the older ones (e.g., Rana 1991; Pagel 1997 and references therein); this implies a slow infall, on a timescale larger than implied by the old data (larger than the $\sim$3–4 Gyr timescale for an exponentially decreasing infall adopted in, e.g., PA95).

The simple model described in § 2 can reproduce the above constraints, provided that the various parameters are adjusted as follows:

A. The infall rate $f(t)$ is normalized to the local disk density Σ_T: $\int_0^T f(t)dt = \Sigma_T$, where $T = 13.5$ Gyr is the adopted age of the disk.

B. The form of $f(t)$ is adjusted to satisfy the constraint of the G-dwarf metallicity distribution. Although an exponentially decreasing infall rate with a timescale of $\tau > 7$ Gyr can provide a satisfactory fit to the new data (e.g., Chiapini, Matteucci, & Gratton 1997), we adopt here a Gaussian form for the infall rate,

$$f(t) = \frac{1}{\sqrt{2\pi}\sigma} e^{(t-t_0)^2/2\sigma^2}, \quad (1)$$

with $t_0 = 5$ Gyr and a width of $\sigma = 5$ Gyr. The physical motivation for such a choice is that because of its small initial surface density, the local disk initially accretes a small amount of the surrounding gas; as the disk mass and gravitational potential build up, the accretion rate gradually increases, but starts decreasing when the gas reservoir is depleted. Obviously, this form for the infall rate is by no means unique; other prescriptions may do as well. We note, however, that such long timescales for disk formation (many Gyr) are also obtained in chemodynamical models (Samland et al. 1997).

C. The coefficient of the adopted SFR is 0.1, i.e., $\Psi = 0.1\ \Sigma_G^{1.5}\ M_\odot\ \mathrm{pc}^{-2}\ \mathrm{Gyr}^{-1}$. Combined with the adopted infall rate, this leads to a current gas surface density of $\Sigma_G \sim 10\ M_\odot\ \mathrm{pc}^{-2}$ and to a final stellar surface density of $\Sigma_* \sim 40\ M_\odot\ \mathrm{pc}^{-2}$, both compatible with the observations. Note that with the adopted infall and star formation rates, a current SFR $\sim 3\ M_\odot\ \mathrm{pc}^{-2}\ \mathrm{Gyr}^{-1}$ is obtained at $T = 13.5$ Gyr, again in agreement with observations. Finally, these ingredients, combined with the adopted IMF and stellar yields (§ 2), lead to a local metallicity close to the solar one 4.5 Gyr ago and slightly higher today.

D. The SN Ia rate is adjusted to reproduce the observed decline of O/Fe in the local disk. The introduction of this delayed Fe source leads to an age-metallicity relationship somewhat steeper at late times than (but still compatible with) the observations.

Summarizing the above conditions, one can say that the problem of the chemical evolution of the local disk is well determined and overconstrained, since the number of adjustable parameters (A–D) is smaller than the number of observational constraints (1–5).

The results of the adopted model and the comparison to observations are shown in Figure 1. It can be seen that all observational constraints are satisfactorily reproduced. We emphasize that this solution is by no means unique (see Tosi 1988), i.e., some other combination of the input parameters may also lead to acceptable results. Note, however, that the constraints are relatively tight and do not allow for a wild variation in the input parameters. In particular, the metallicity distribution strongly suggests slow formation of the local disk; this is corroborated by the observed current local SFR, which is not very different from the past average one (PASFR $= \Sigma_*/T \sim 4\ M_\odot\ \mathrm{pc}^{-2}\ \mathrm{Gyr}^{-1}$). A very high early SFR declining to very low current values is not compatible with these data.

Having fulfilled the main observational constraints, the model can then be used with some confidence for other astrophysical applications. One such application appears in the lower middle panel of Figure 1. The evolution of deuterium shows that this fragile isotope produced in the big bang can only be destroyed by a factor of $\sim$2 in this kind of model. Its inferred pregalactic abundance cannot then be much higher than D/H $\sim 4 \times 10^{-5}$, in agreement with the observations of Tytler and collaborators in high-redshift gas clouds (Burles & Tytler 1998 and references therein), but in disagreement with the high values reported by other groups (see Hogan 1998 for a review of all the measurements). Similar conclusions are reached in several other studies of the evolution of the local disk that reproduce all the major observational constraints (e.g., Tosi 1998 and references therein). The low D/H pregalactic values alleviate (but do not solve) the problem of ^{3}He overproduction, which is definitely a problem of stellar nucleosynthesis, not Galactic evolution (e.g., Prantzos 1996; Tosi 1998).

3.2. *The Milky Way Disk*

Contrary to the case of the solar neighborhood, the available observations for the Milky Way disk offer information mainly about its current status, not its past history. The main relevant observables are (PA95; Pagel 1997; and Fig. 2):

1. The total mass of gas and stars in the disk ($\sim 8 \times 10^9\ M_\odot$ and $\sim 5 \times 10^{10}\ M_\odot$, respectively), the total current SFR ($\sim$3–5 $M_\odot\ \mathrm{yr}^{-1}$), and the current supernova rates ($\sim$1.5 SN II century^{-1} and $\sim$0.4 SN Ia century^{-1}, respectively, as suggested by observations of Sbc type spirals; see Tammann, Loefler, & Schroder 1994 and Cappellaro et al. 1997). Note that these quantities are often mentioned as constraints to (and predictions of) one-zone models of the Galaxy, which are presumed to reflect the evolution of the whole disk. This is obviously wrong, since the disk is a heterogeneous system, as suggested by the observed gradients (see points 3–6 below). A multizone model with different SFR histories in its various zones should be used.

2. The current gas profile, dominated by the molecular ring at Galactocentric distance of $R \sim$ 4–5 kpc and by H I of roughly constant surface density at distances of 6–14 kpc (Dame 1993).

3. The stellar profile, which decreases outward exponentially. The value of the characteristic scale length is still under debate, but recent studies converge toward low scale lengths, around 2.5–3 kpc (Sackett 1997). The combination of observables (2) and (3) leads to a gas fraction profile that decreases steeply in the inner disk, suggesting that the star formation efficiency has been greater in those regions than in the outer disk.

4. The current SFR profile (traced by the surface density of pulsars and supernova remnants or the Hα emissivity profile), which strongly decreases outward (Wang & Silk 1994 and references therein). Note that the SFR profile does

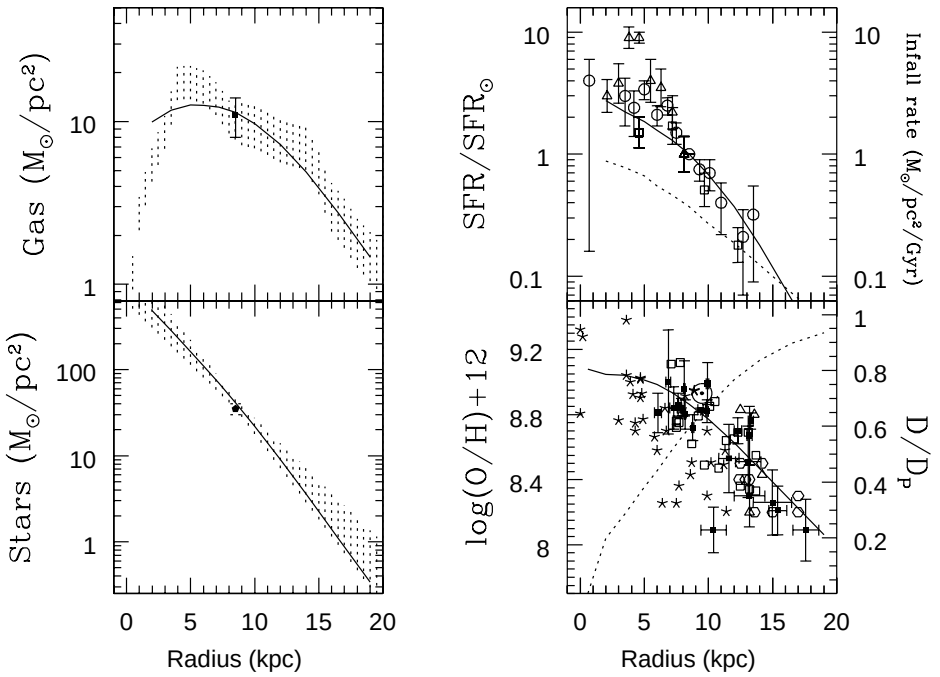

FIG. 2.—Results of a simple (independent-ring) model for the chemical evolution of the Milky Way disk at a Galactic age $T = 13.5$ Gyr, with a comparison to observations. The adopted SFR is $\Psi(R) \propto \Sigma_G^{1.5}/R$, and the adopted infall rate is Gaussian in time, with $\Delta\tau = 6$ Gyr in all the zones. The peak t_0 of the Gaussian depends on the Galactocentric radius, and is $t_0 = 2$ Gyr at $R = 2$ kpc and $t_0 = 6$ Gyr at $R = 18$ kpc. *Left panels*: final profiles of the surface density of gas (*top*) and stars (*bottom*). Solid lines show model results; shaded regions correspond to observations for the disk, and data points with error bars at Galactocentric distance $R_0 = 8.5$ kpc correspond to values in the solar neighborhood. *Top right panel*: current profiles of SFR (*solid line, scale on the left*) and infall (*dotted line, scale on the right*) in the Milky Way disk, according to our model. The SFR profile is normalized to its local value at $R_0 = 8.5$ kpc, and should be compared to observations (data from Prantzos & Aubert 1995). *Bottom right panel*: Current abundance profiles of oxygen (*solid line, scale on the left*) and deuterium (*dotted line, scale on the right*). The deuterium abundances are normalized to the primordial value D_P and suffer small depletions in the solar neighborhood (a factor of ~ 2), but much larger ones in the inner disk (factors of > 20 in the central regions). Data for O are from H II regions: *open squares*, Shaver et al. (1983); *open hexagons*, Vilchez & Esteban (1996); *open triangles*, Fich & Silkey (1991); *asterisks*, Afflerbach et al. (1997); and from B stars: *filled symbols*, Smartt & Rolleston (1997).

not follow the molecular or the total (molecular + atomic) profile, i.e., the SFR is not simply proportional to some power of the gaseous profile.

5. The current metallicity profile, usually traced by oxygen observed in H II regions (Shaver et al. 1983; Vilchez & Esteban 1996) and planetary nebulae (Allen, Carigi, & Peimbert 1998), and showing a gradient of $d[\mathrm{O/H}] \sim -0.08$ dex kpc^{-1}. Observations of O abundances in young, B-type stars in the early 1990s suggested a surprisingly flat oxygen abundance profile; the controversy seems to have been settled by a recent non-LTE treatment of these objects (Smartt & Rolleston 1997), confirming the gradient in H II region abundances.

6. Current abundance profiles of other elements (e.g., N, S, etc.) and isotopic ratios (such as ^{12}C/^{13}C, ^{16}O/^{17}O). However, the constraints imposed by these observables are either similar to those already imposed by the oxygen profile or much more sensitive to the adopted nucleosynthesis prescriptions (concerning, e.g., the primary and/or secondary origin of N and ^{13}C, the stellar production of ^{3}He, etc.) than to the chemical evolution model itself.

Note that since there are essentially no constraints on the past history of the Milky Way disk (i.e., no age-metallicity relations or metallicity distributions are available for other regions), there is much more freedom in constructing a model than is the case for the solar neighborhood. Still, it is meaningful to construct models, insofar as the number of parameters used is considerably smaller than the constraints listed as (1)–(5) above.

These constraints make the Milky Way disk a "test bed" for theories of star formation in disk galaxies. Indeed, several ideas have been put forward over the years for a radial dependence of the star formation efficiency, most of them on the basis of various instability criteria for gaseous disks (Talbot & Arnett 1975; Wyse & Silk 1989; Dopita & Ryder 1994; Silk 1997). Star formation theories also exist and can be tested for disk galaxies, rather than for, e.g., ellipticals or irregulars.

Up to now, these theoretical prescriptions have been used or tested only in the framework of extremely schematic models, considering the disk as a system of independent (one-zone) rings (Matteucci & François 1989; Wyse & Silk 1989; Wang & Silk 1994; PA95; Ferrini et al. 1994; Carigi 1996). This oversimplification generally ignores the possibility of radial inflows in gaseous disks produced, e.g., by viscosity or by the infall of gas with a specific angular momentum different from that of the underlying disk; in both cases, the resulting redistribution of angular momentum leads to radial gas flows. The magnitude of the effect is difficult to evaluate, because of our poor understanding of viscosity and our ignorance of the kinematics of the infalling gas. Models with radial inflows have been explored in the past (Mayor & Vigroux 1981; Lacey & Fall 1986; Clarke 1989; Chamcham & Tayler 1994); at the present

stage of our knowledge, the introduction of radial inflows in the models would imply even more free parameters and effectively negate any possibility of studying the radial variation in the efficiency of the SFR.

Note that a radial variation of the infall timescale (in the framework of the simple independent-ring model) may play a similar role. To give an example, a disk galaxy may be formed inside-out in either of two ways: (1) with a constant efficiency of the SFR and an infall much more rapid in the inner zones than in the outer ones, or (2) with the same infall timescale throughout the disk and a SFR efficiency that is radially decreasing outwards. In other words, the possibility of a radially varying infall timescale makes it difficult to unambiguously test theories of the radial variation of the SFR efficiency (and vice versa). Only full-scale chemodynamical evolution models could help break this degeneracy. Although such models exist (Steinmetz & Muller 1994; Samland et al. 1997), they are limited in various aspects (e.g., the instantaneous recycling approximation is always assumed), and cannot yet be checked against all available observational data.

Despite the degeneracy of the problem, simple toy models can often give useful insights into the above questions. In addition, once a successful (albeit nonunique) model is obtained, it can be used to test some nucleosynthesis prescriptions (resulting in radial variations of the primary or secondary elemental or isotopic ratios), or even to make further predictions (e.g., Prantzos et al. 1996 on the gradients of the CO isotopes).

In this work we adopt an independent-ring model for the disk, as has been used in several previous studies. The adopted star formation rate is

$$\Psi(R) = 0.1\Sigma_G^{1.5}\left(\frac{R}{R_\odot}\right)^{-1} M_\odot \text{ pc}^{-2} \text{ Gyr}^{-1}, \qquad (2)$$

based on the idea that stars are formed in spiral galaxies when the interstellar medium with angular frequency $\Omega(R)$ is periodically compressed by the passage of the spiral pattern, having a frequency $\Omega_P = \text{const.} \gg \Omega(R)$. This leads to SFR $\propto \Omega(R) - \Omega_P$, and for disks with flat rotation curves, to SFR $\propto R^{-1}$ (Wyse & Silk 1989). On the other hand, a Gaussian infall with half-width $\sigma = 5$ Gyr is adopted over the entire disk, to account for the G-dwarf problem in the solar neighborhood (eq. [1]). To simulate the inside-out formation of the disk (suggested by dynamical models, e.g., Larson 1976; Samland et al. 1997), the maximum infall time t_0 in equation (1) is assumed to be radially dependent, taking on lower values in the inner regions ($t_0 = 2$ Gyr at radius $R = 2$ kpc) and larger ones in the outer disk ($t_0 = 6$ Gyr at $R = 18$ kpc). The integral over time of the infall rate $f(t, R)$ is normalized to the current total mass profile: $\int_0^T f(t, R)dt = \Sigma_T(\text{R})$. The radial variation in the SFR efficiency and in the infall peak time t_0 are the only new parameters introduced in the model, all others being already fixed by the model of the solar neighborhood (§ 3.2). Note that the form of the adopted SFR law is somewhat different from the one adopted in PA95, where it was found that $\Psi \propto \Sigma_G/R$ produces a relatively flat current O gradient in the outer disk, in agreement with the observations of B stars at that time (circa 1995). However, the reanalysis of the B-star data by Smartt & Rolleston (1997) reveals an important gradient in the whole disk (in agreement with other traditional tracers, including H II regions and planetary nebulae), and requires a steeper radial dependence of the SFR, such as the one adopted here.

It turns out that with this simple parametrization, our model reproduces reasonably well the constraints (1)–(5), as can be seen in Figure 2. Among these, the gaseous profile is the most difficult to reproduce in models of this kind; we obtain a rather broad peak around 6 kpc, in rough agreement with observations. The model also reproduces quite well the total current SFR and supernova rates (Fig. 3, *left panel*), as well as various other quantities. This is a rather encouraging success, since the number of new constraints is much larger than the number of new parameters introduced; the model can then be used with some confidence for making further predictions.

One of the most important results of this type of model concerns the evolution of deuterium. We find that the final abundance profile of deuterium shows a significant gradient, much larger in the inner regions than (and anticorrelated with) that of oxygen. The reason for this is that while all stars deplete deuterium (especially the numerous low-mass stars), only massive stars produce oxygen. In regions with a large, early SFR (as in the inner disk), low-mass stars become the major actors in the late stages of chemical evolution, ejecting D-free and O-free material; as a result, the abundance of D continues to decrease, while the abundance of O saturates (and may even decrease, if not augmented by production from the relatively few massive stars that are born at late times). Thus, the D abundance profile, which is not subject to saturation effects, is the most sensitive tracer of the past SFR history of the disk, especially in the inner regions (Prantzos 1996). Radio measurements of the D abundance in the outer disk have recently been reported by Chengalur, Braun, & Burton (1997), who find D/H $= 3.9 \pm 1 \times 10^{-5}$, i.e., compatible with a low primordial D (since any significant D depletion is utterly implausible in the outer disk regions, where the large gas fraction and the low metal content suggest a reduced star formation efficiency). Further progress is expected with the *Infrared Space Observatory* satellite and the forthcoming *Far-Ultraviolet Spectroscopic Explorer*-LYMAN mission.

3.3. *The Galactic Bulge*

The number of available observational constraints on star formation is much smaller in the bulge of our Galaxy than in the disk. However, we also consider the evolution of the bulge here, since it represents an important fraction of the total visible mass of the Milky Way ($\sim 10^{10}$ $M_\odot$, or $\sim$20% of the total). Both observations and theory suggest that the bulge was formed on a rather short timescale, on the order of 1 Gyr. This implies that the bulge SFR may have dominated the SFR of the young Milky Way, as shown in recent dynamical simulations (Samland et al. 1997).

The main observational constraints for the bulge are summarized in McWilliam & Rich (1994) and Pagel (1997). The metallicity distribution of K giants observed in the Baade window peaks at the same [Fe/H] as the local G-dwarf metallicity distribution, but it has a larger population in the low-metallicity range. It is not clear whether this is compatible with the predictions of a closed-box model or whether it represents a "K-giant problem" analogous to the G-dwarf problem in the solar neighborhood. The behavior of the [α/Fe] ratios is quite puzzling: while Si/Fe and Ca/Fe behave as in the solar neighborhood

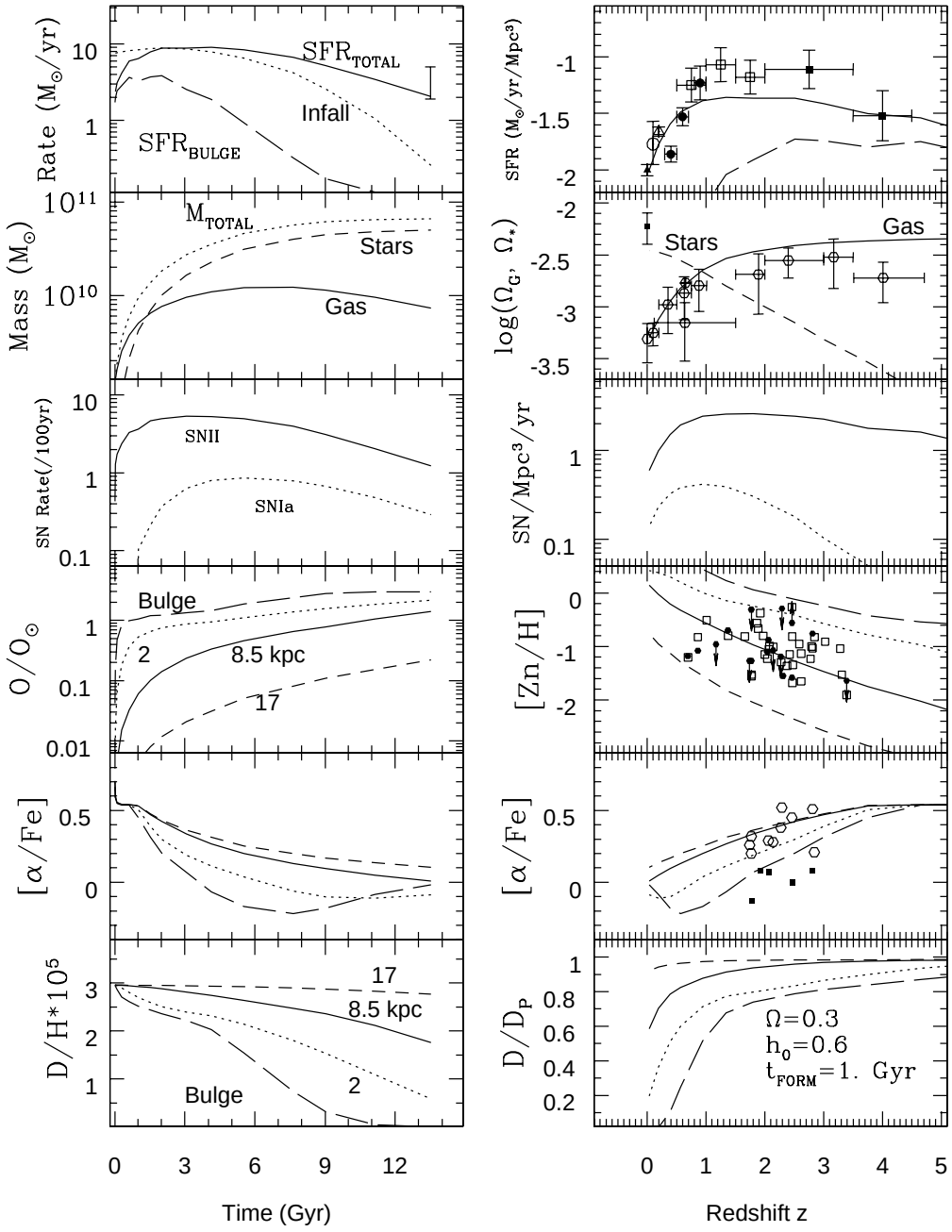

FIG. 3.—History of the Milky Way disk as a function of time (*left panels*) and redshift (*right panels*), assuming that our Galaxy is a typical spiral, and adopting a cosmological model with $\Omega = 0.3$, $h_0 = 0.6$, and galaxy formation starting 1.0 Gyr after the big bang. *Left panels*: from top to bottom, history of (1) total (disk + bulge) SFR, bulge SFR, and total infall rate; (2) gaseous, stellar, and total mass; (3) SN II (*solid line*) and SN Ia (*dotted line*) rates; (4) overall metallicity in four different zones, at distances of 2, 8.5, and 17 kpc from the Galactic center and in the bulge; (5) [*a*/Fe] ratio in the same zones; and (6) D abundance in the same zones. *Right panels*: from top to bottom, (1) the "cosmic" SFR of disk galaxies, which when normalized to the current local value ($z = 0$) does not show the steep observed increase back to $z \sim 1$ (although it peaks at $z \sim 1$, as do observational data). Other galaxy types (perhaps ellipticals?) should account for the discrepancy between theory (*solid line*, total SFR; *dashed line*, bulge SFR) and observations; data from Madau (1997). (2) Evolution of gas and star densities; data for neutral gas (H I + 25% He; *open symbols*) from Natarajan & Pettini (1997), data for local star density (*filled symbols*) from Briggs (1997). (3) cosmic evolution of SN II and SN Ia rates. (4) The evolution of metallicity, traced by Zn, in various regions of spiral disks (the same regions as on the corresponding panel on the left) brackets well the observed abundances of Zn/H in Lyα absorbers; data from Pettini et al. (1997) (*open symbols*) and Lu et al. (1996) (*filled symbols*); those systems may well be (proto)galactic disks. (5) The [α/Fe] ratio in these same zones declines smoothly from its initial value of $\sim$0.5 at high *z* (due to SN II) to approximately solar values (due to Fe produced by SN Ia), at a rate depending on the corresponding SFR; data for Si/Fe from Lu et al. (1996) (*open symbols*, neglecting dust depletion) and Vladilo (1998) (*filled symbols*, corrected for dust effects). (6) The corresponding evolution of D shows that considerable depletion may take place in the inner disk regions, but only at low redshifts; abundances measured at high redshifts should be close to the primordial value.

(declining in the [Fe/H] > -1 range), Mg/Fe and Ti/Fe remain $\sim$constant $\sim$3 times the solar value. The implications of these results for nucleosynthesis (from both SNe II and SNe Ia) during the bulge evolution are not clear. No indications of a substantial abundance gradient exist, at least in the inner kiloparsec, where most of the bulge mass resides. Finally, note that the largest observed metallicity is closer to $\sim 3\,Z_\odot$ than $> 5\,Z_\odot$, as claimed in the past.

We adopt here a simplified one-zone model for the evolution of the bulge, not very different from that of Matteucci & Brocato (1990). The bulge is assumed to occupy the inner 2 kpc of the disk. It is formed by Gaussian infall on a timescale of 2 Gyr and evolves with an enhanced SFR efficiency, ~ 20 times that in the solar neighborhood; with a peak SFR of $\sim 5\ M_{\odot}\ \mathrm{yr}^{-1}$, it dominates the Galactic SFR for a few Gyr. At the end of that period, the bulge has a total mass of $10^{10}\ M_{\odot}$, with a final gas fraction $\sim 10^{-3}$ and a final metallicity of $\sim 3\ Z_{\odot}$. The resulting metallicity distribution contains more metal-poor stars than the corresponding one in the solar neighborhood, in rough agreement with the observations. Deuterium has been considerably depleted, by more than a factor of 30 from its initial value. Although this is by no means a detailed bulge model, it suffices for the requirements of this work, concerned with the evolution of the Milky Way in a cosmological context.

4. IMPLICATIONS FOR COSMIC CHEMICAL EVOLUTION

In recent years, observations of high-redshift systems have begun to reveal some aspects of the early phases of chemical evolution in the universe. These observations concern the global SFR and H I content of the universe (i.e., both averaged over sufficiently large volumes), as well as the abundances of various elements in gaseous systems in the line of sight of quasars. To these one should add, in principle, observations of D abundances, although the current status of these observations (e.g., Burles & Tytler 1998) does not allow the establishment of a trend as a function of redshift. More specifically, the available observations concern:

1. *The comoving luminosity density of the Universe*, from the present epoch (redshift $z = 0$) back to $z \sim 4$, in several broad passbands (Madau 1998). The data, obtained in various deep spectroscopic and photometric surveys with ground-based telescopes and the *HST*, show a steep rise in the luminosity density from $z = 0$ to $z \sim 1.5$ (by a factor of ~ 10), followed by a slow decline; in fact, the data points at high redshift should be considered only as tentative, since possible obscuration by dust could hide large numbers of UV-emitting stars (Guiderdoni et al. 1998). In principle, the UV luminosity traces the underlying massive star population and (assuming a universal stellar IMF) the corresponding SFR. In practice, the method has several limitations (Madau 1997), but it can still give a rough idea of the evolution of the SFR on a cosmic scale, at least at late times.

2. *The comoving density of neutral gas in Lyα absorbers*, taking into account the observed column density distribution of these systems as a function of redshift (Storrie-Lombardi, McMahon, & Irwin 1996; Natarajan & Pettini 1997). The data show an increase in the gas density back to $z \sim 2$ (by a factor of ~ 3), then a flattening at a value roughly comparable (within a factor of ~ 2) to that of the stellar density in the local universe. This could indicate that the bulk of star formation took place after $z \sim 2$, a conclusion corroborated by observable (1) above. Note, however, the absence of information about the amounts of molecular and ionized gas, which could modify this conclusion.

3. *The gas-phase abundances of several elements in a few dozens of damped Lyα absorbers (DLAs) at various redshifts* (Lu et al. 1996; Pettini et al. 1997). There is an overall trend of decreasing metallicity with increasing redshift, but also a large dispersion at all redshifts. Values range between 1/10 and 1/300 solar, while an average metallicity of [Fe/H] $\sim$ 1/30 solar is derived in the redshift range $2 < z < 3$. However, the possibility of dust depletion does not allow us to use most of these metals as reliable tracers of the metal content of the gas, with the possible exception of Zn (which is less refractory than most of the other observed elements, see § 4.2).

The observables listed in (1)–(3) above have prompted several studies of cosmic chemical evolution (e.g., Pei & Fall 1995). In most cases, a simple model of chemical evolution is adopted (i.e., a one-zone model assuming an IMF and a SFR, as well as the possibility of inflows and outflows) and assumed to be representative of a sufficiently large volume of the universe; obviously, the total amount of gas in the box (processed in the system *and* participating in inflows/outflows) corresponds to the total baryon content of that representative volume. The predictions of the model concerning the gas and metal content as a function of time are then translated into functions of the redshift (in the framework of a given cosmological model) and compared to observables (2) and (3).

Note, however, that although observables (1) and (2) can be considered truly global (if the possibility of hidden star-forming regions and large amounts of molecular and ionized gas is neglected), observable (3) is rather local; indeed, it traces the metallicity of only those systems that have still retained some gas at a given redshift. The metals produced, e.g., early-on in ellipticals, and already incorporated in their stars or expelled as ionized gas in the intergalactic medium of galaxy clusters, do not appear in the census of (3). The predictions of a global model for the evolution of the metallicity cannot then be directly compared to the observations in (3).

Since the only system with data sufficient to constrain its history is the Milky Way, it is of great interest to see how its evolution, translated into a cosmological setting, compares to the above observables (1)–(3) of cosmic evolution. This exercise has previously been performed by several groups. In some cases, the observed abundance patterns of our Galaxy (notably the age-metallicity relationship for the local disk and the α/Fe ratio versus Fe) are compared to the abundance data of DLAs (e.g., Timmes et al. 1996). On the basis of such a comparison, Lu et al. (1996) and Pettini et al. (1997) conclude that DLAs are (probably) not the precursors of Milky Way–type disks. A similar conclusion is reached by Vladilo (1998), who takes into account dust depletion for a number of elements.

A somewhat different approach is adopted in Fritze-von Alvesleben (1997), who uses a simple one-zone model for the evolution of various early- and late-type spirals, and suggests that galactic disks, forming stars at different rates, may well account for the observed evolution of metallicity in DLAs. On the other hand, Ferrini, Molla, & Diaz (1997) compare the predictions of a multizone model for the Milky Way to the metallicity versus redshift data of Lu et al. (1996) and Pettini et al. (1997). They conclude that the range of metallicities spanned during the evolution of the Milky Way disk is compatible with what is observed.

Our own approach is similar to that of Ferrini et al. (1997), but we also consider the evolution of the SFR and gaseous content (as in, e.g., Pei & Fall 1995), supernova

rates, α/Fe ratios, and deuterium. All of these quantities constitute important probes of the chemical evolution on a cosmic scale. Of course, we do not expect that the evolution of the Milky Way matches all available data on DLAs. A favorable comparison would imply that the Milky Way is a truly average galaxy, but this would be a rather improbable result. Rather, the aim of our comparison is to see to what extent the Milky Way evolution differs from the average model (Prantzos 1998a).

The results of our model are shown in Figure 3. In the left-hand panel we display the results of the model as a function of Galactic time, showing the total SFR, bulge SFR, and total infall rate; the total, stellar, and gas mass; supernova rates for SN Ia and SN II; metallicity in the bulge and at several Galactocentric distances ($R = 2$, 8.5, and 17 kpc, respectively); α/Fe ratios in the same regions; and deuterium abundance in the same regions. As discussed in detail in § 3, these results are in satisfactory agreement with the available observational constraints.

4.1. *Cosmic SFR, Stellar and Gaseous Content of the Universe*

In the right-hand panel, the same results are plotted as a function of redshift z in a cosmological model with $\Omega = 0.3$ and $H_0 = 60$ km s^{-1} Mpc^{-1}, adopted here for illustrative purposes. The adopted time delay between the big bang and the time of galaxy formation is $\Delta t = 1$ Gyr. Variations of these parameters do not significantly change our results at low z; at high z, the effects of varying Δt are quite important (e.g., Timmes et al. 1995a), but we are not too concerned with this regime, since observations are quite uncertain.

In order to compare the evolution of the Milky Way SFR to the cosmic history, we assume that Milky Way–type spirals dominate the current cosmic SFR. We then normalize the model SFR at Galaxy time $T = 13.5$ Gyr, or cosmic time $\tau = T + \Delta t = 14.5$ Gyr ($\Psi_0 \sim 2\ M_\odot$ yr^{-1}), to the observed cosmic SFR at $z = 0$ (for which we adopt the data point of Gallego et al. 1995, as corrected by Madau 1997; $\psi_0 \sim 10^{-2}\ M_\odot$ yr^{-1} Mpc^{-3}). It can be seen that the Milky Way SFR does not increase between $z = 0$ and $z \sim 1$ as steeply as indicated by observations of the cosmic SFR, although it peaks at about the right redshift. Milky Way–type spirals can then only partially account for the observed evolution of the cosmic SFR, contributing about 30%–40% at $z \sim 1$; this is a reasonable conclusion, since other galaxy types (ellipticals? mergers? starbursts? dwarfs?) are also expected to make a large contribution to the cosmic SFR at $z \geq 1$. Note that the bulge SFR dominates the Galactic SFR between the highest redshifts and $z \sim 4$ (at least in the framework of this type of model).

With the normalization adopted for the cosmic SFR, we find that during their evolution spiral galaxies have produced a total current star density of $\rho_*(z = 0) \sim 2.5 \times 10^8\ M_\odot$ Mpc^{-3}, which corresponds to a model $\Omega_{*,\mathrm{mod}}(z = 0) = \rho_*/\rho_c \sim 0.003$ (a value of $\rho_c = 7 \times 10^{10}\ M_\odot$ Mpc^{-3} is adopted for the critical density). On the other hand, observations show that in the local universe, $\Omega_{*,\mathrm{obs}}(z = 0) \sim$ 0.004–0.008 (e.g., Briggs 1997). This means that spirals evolving according to our model can produce between ~30% and up to 75% of the stellar content of the universe.

Adopting this same normalization, we can then translate the history of the gaseous and stellar content of the Milky Way into a cosmological setting (Fig. 3). We find that the current gas content obtained from the model [$\rho_G(z = 0) \sim 3.5 \times 10^6\ M_\odot$ Mpc^{-3}, corresponding to $\Omega_{G,\mathrm{mod}} \sim 4.5 \times 10^{-3}$] is very close to its observed value at $z = 0$ ($\Omega_{G,\mathrm{obs}} \sim 5 \times 10^{-3}$; Briggs 1997); the gas left in spirals today according to this model is sufficient to explain the observed gas amounts in the local universe. In other words, if Milky Way–type spirals dominate star formation in the local universe (a plausible assumption), and if their evolution is described by the simple model of § 3 (not an implausible assumption), then spirals should today contribute $\Omega_* \sim 3.5 \times 10^{-3}$ and $\Omega_G \sim 4.5 \times 10^{-4}$; both values are in agreement with observations.

On the other hand, our model fits the observations of both the cosmic SFR *and* the gas content at $z < 1$. This means that if there are important quantities of hitherto undetected gas at low z (a rather improbable scenario; see Natarajan & Pettini 1997), they should not participate in the cosmic SFR. At higher redshifts the situation is different, since our model requires larger amounts of gas than observed at $z \sim 3$. Taking into account the fact that our model describes only the formation of spirals, but not of ellipticals, this implies that even larger gas amounts should be present at these high redshifts, in either molecular or ionized form.

Finally, in the third panel of Figure 3 we present the evolution of the SN II and SN Ia rates in the Milky Way (*left panels*) and the corresponding rates as a function of redshift (*right panels*). The former are expressed in units of SN century^{-1}, and it can be seen that the current values are compatible with those estimated for the Milky Way (i.e., ~1.5 SNe II/Ibc century^{-1} and ~0.4 SNe Ia century^{-1}; see § 3.2). The latter are expressed as SN Mpc^{-3} yr^{-1}, and their normalization stems from that of the cosmic SFR (see above). The SN II rate is obviously proportional to the SFR, but the interesting point here is the derived evolution of the SN Ia rate as a function of redshift. SNe Ia are extremely important as distance indicators in the universe, and their detection at high redshifts is the main object of the Supernova Cosmology Project, the first results of which have recently been reported (Pain et al. 1996). In several recent works, the cosmic evolution of the SN Ia rate is studied on the basis of some ad hoc formula for the SN Ia rate as a function of the SFR and other parameters (e.g., Madau 1998; Sadat et al. 1997; Ruiz-Lapuente & Canal 1998). In contrast, our study links the evolution of the SN Ia rate to an observable, i.e., the decline of the O/Fe ratio in the local disk (see § 3.1), and thus is presumably closer to reality, at least as far as disk galaxies are concerned. Since SNe Ia are also observed in ellipticals, our curve of the cosmic SN Ia rate (normalized in the same way as the SN II and SFR curves) gives a strict lower limit to the expected frequency of SNe Ia as a function of redshift.

4.2. *History of Elemental Abundances in DLAs*

Despite several papers on the evolution of metallicity in DLAs (e.g., Timmes et al. 1995a; Malaney & Chaboyer 1996; Lu et al. 1996; Pettini et al. 1996), the situation is still far from clear. From the observational point of view, most of the detected elements are known to be refractory, and they are expected to be depleted onto dust grains to various extents. The "observed" abundances should then be interpreted as lower limits rather than as real values, making a meaningful comparison with theoretical predictions difficult. This concerns iron in particular, an element with a rather well understood nucleosynthesis history, and found

to be heavily depleted in the ISM of our Galaxy (e.g., Savage & Sembach 1996). The observed behavior of [Fe/H] in DLAs as a function of redshift thus cannot be directly compared to, e.g., the age-metallicity relationship in the solar neighborhood; such a comparison might lead to erroneous conclusions, (e.g., Lu et al. 1996, Pettini et al. 1997, and Ferrini et al. 1997).

Among the observed elements in DLAs, Zn is the least affected by dust depletion; its observed abundance should not be very different from the true value. However, from the theoretical point of view, the nucleosynthesis of Zn is not well understood. The only known production site is massive stars, and the most detailed models of this site are those of WW95, who give the only available models with yields of the various isotopes as a function of initial stellar metallicity. The Zn yields of these models show an unexplained behavior; the dominant Zn isotope, ^{64}Zn, is underproduced, while the yields of the next two more important isotopes, ^{66}Zn and ^{68}Zn, increase strongly as metallicity increases from 0.1 $Z_\odot$ to $Z_\odot$. The reason for this behavior in the models is not yet well understood. As a result, the [Zn/Fe] ratio calculated with the metallicity-dependent yields of WW95 and a chemical evolution model shows a rather abrupt and pronounced increase for metallicities [Fe/H] > -1, while it stays nearly constant at lower metallicities (Timmes et al. 1995b). This behavior is not found in the observed pattern of the Zn/Fe ratio; both halo and disk stars of all metallicities show solar Zn/Fe (see Timmes et al. 1995b and references therein), despite the fact that SNe Ia, the main Fe producers in the disk, do not produce significant Zn amounts.

This situation does not allow us to trust theoretical nucleosynthesis prescriptions for the evolution of Zn, since theory seems unable to reproduce observations in the Galaxy. Therefore, we adopt an empirical approach for the nucleosynthesis of Zn, as already suggested in Timmes et al. (1995a); based on the observed Zn/Fe pattern in the Galaxy, we assume that Zn traces Fe at all metallicities. Since the history of Fe in the Galaxy is observationally well constrained (at least in the solar neighborhood) and reasonably well reproduced by our models, we translate our model results for [Fe/H] as a function of redshift and compare them to observations of [Zn/H] in DLAs (assuming that Zn is the most reliable metallicity tracer in those systems).

The results (see Fig. 3) show that during its evolution the disk spans a metallicity range that is fully compatible with observations. Inner regions with enhanced SFR efficiency have larger metallicities than the outer regions by factors of $\sim$10–30. The abundances of the model for bulge-type regions are always higher than the observed ones, while abundances corresponding to the local disk are close to the average metallicity for $3 > z > 1$. Note that for geometrical reasons, the probability of detecting outer disk regions is higher, favoring systematically lower abundances than those spanned during the local history.

The recent work of Ferrini et al. (1997) is based on similar ideas, adopting a multizone model for the evolution of the Galaxy and comparing the results for the various zones to observations. However, it leads to somewhat different conclusions, since the theoretical predictions are compared to Fe, not Zn, in DLAs. It is found that these systems have a metallicity history unlike the one of the local disk, their abundances being systematically lower than the local ones. The same conclusion, i.e., that DLAs are probably not rotating disks, was reached in Lu et al. (1996) and Pettini et al. (1997), based on the observed age-metallicity relationship of the solar neighborhood (where metallicity is measured by Fe). On the contrary, our work shows that, *if* Zn is a reliable metallicity tracer in DLAs and *if* it always traces Fe, as in the Galaxy, then the metallicity evolution of DLAs corresponds fairly well to that of Milky Way–type spirals.

It has been suggested that the abundance ratios in DLAs could help identify them as galactic haloes, protodisks, dwarf galaxies, etc. For instance, halo stars in our Galaxy have [α/Fe] $\sim$ 0.5 (where α stands for O, Mg, Si, S, Ca, Ti), while disk stars have lower values and solar-type stars have [α/Fe] $\sim$ 0. Although this behavior rather unambiguously characterizes stars in our Galaxy, it is not clear that it helps at all with the identification of DLAs. The reason for this is that in the case of the Milky Way, the decline of α/Fe is attributed to the delayed ($\sim$1 Gyr) action of SNe Ia at a time when the halo evolution is over and no more stars are formed there to be enriched in Fe; in other words, the abundance pattern of halo stars is "frozen" quite early on (>10 Gyr ago). On the other hand, DLAs are observed down to redshifts of $z \sim 1$, i.e., their gas and abundance histories span a large fraction of cosmic time. During that long interval, SNe Ia have certainly had time to pollute the ISM of DLAs with Fe. On theoretical grounds, it seems improbable that we would find DLAs with typical halo patterns, especially at the lowest redshifts (unless the delayed Fe-source interpretation for the decline of Fe in the local disk is wrong).

Despite this, abundance ratios in DLAs could give interesting hints as to their evolution, but evaluation is hindered by dust-depletion effects. Lu et al. (1996) find that the abundance ratios in DLAs are mostly (or entirely) consistent with SN II nucleosynthesis (i.e., halo star patterns), without significant modification by dust depletion. On the other hand, analyzing the same data, Kulkarni, Fall, & Truran (1997) find that dust significantly affects the DLA abundance ratios. Similarly, Vladilo (1998) finds that when dust effects are self-consistently taken into account, the resulting α/Fe ratio is essentially solar at all redshifts.

From the theoretical point of view, the situation is not much better. Although the α/Fe pattern is well known in halo and local disk stars, there is no relevant information for other parts of the disk, and the uncertainty in the SN Ia rate makes it impossible to give reliable predictions for these regions. As for the bulge, observations reveal rather puzzling patterns, as discussed in § 3.3.

For illustrative purposes, in Figure 3 we present the results of our model as a function of galactic time (*left panels*) and redshift (*right panels*). In the framework of the adopted model, the evolution of the halo stops before $z \sim 3$, so the model cannot be compared with the available data. It can be seen that the various disk regions show a rather similar decline in the α/Fe ratio, somewhat slower in the outer disk zones than in the inner ones. This is because the outer zones form stars later than the inner zones (the disk is formed inside-out), and as a result, SNe Ia form even later. The bulge undergoes a much more rapid evolution, leading to subsolar α/Fe ratios, but the metal-poor gas ejected at late times by the numerous long-lived low-mass stars dilutes all abundances and brings this ratio close to solar again. As seen in Figure 3, the difference in the model α/Fe ratios between the various zones increases with decreasing redshift.

In Figure 3 we also plot the observed [Si/Fe] ratio in DLAs, both from the original work of Lu et al. (1996) and as corrected for dust depletion by Vladilo (1998). If dust depletion is neglected, the observed pattern is nicely reproduced by our model; if the evaluation of dust effects by Vladilo (1998) is correct, then the DLA α/Fe ratio is too low with respect to the model results for all of the galactic zones. In the latter case, various alternatives could be considered: (1) DLAs are indeed protodisks, but the SN Ia rate is not correctly evaluated, except in the solar neighborhood (where the observed decline of α/Fe is well reproduced); (2) DLAs are not protodisks and have evolved in a way different from that described here. In both cases, however, SNe Ia should play an important role at early times.

Finally, in the last panel of Figure 3 we plot our results for the evolution of D in the various zones of our model, as a function of galactic time (*left panels*) and redshift (*right panels*); in the latter case, the depletion factor D/D_P (where D_P is the unknown primordial D abundance) is plotted. It is shown that D can be considerably depleted in the inner galactic zones, but only at very late times or low redshifts. This is because the main agent of D depletion is the numerous low-mass long-lived stars. If the IMF is truly universal, then D abundances observed at high redshifts should be very close to the primordial values, since even an extremely strong early SFR cannot lead to a rapid D depletion. The recently observed discrepant D/H values in high-redshift clouds cannot then be simultaneously explained, i.e., one cannot invoke a high universal primordial value and a strong local depletion to reconcile the discrepant data; one of the values must be wrong. This conclusion can be invalidated by a nonuniversal IMF (truncated from below at 2–3 $M_\odot$) or a nonuniversal primordial D abundance. As discussed in § 3.1, the local disk evolution suggests that the simplest solution of the puzzle is the assumption of a low primordial D.

5. CONCLUSIONS

The basic points of this work can be summarized as follows:

1. We have developed a detailed model for the chemical evolution of the Milky Way disk that reproduces all of the major observational constraints with a minimal number of free parameters. Among these constraints, the recent observations of the local G-dwarf metallicity distribution suggest a slow formation of the local disk (on timescales >6 Gyr) and a correspondingly smooth evolution of the SFR. Successful models of the local disk suggest only small depletion factors of D ($\sim$2–3) and favor low primordial values of that isotope.

2. Observations of various gradients in the Milky Way disk (gas fraction, SFR, metal abundances) suggest a high SFR efficiency in its inner regions; the global Galactic SFR is, however, a smoothly varying function of time, as is the SFR of the local disk. Simple toy models that reproduce the observations reasonably well predict an important D gradient in the inner disk; when measured by forthcoming experiments, the D profile will provide invaluable information on the past history of the disk.

3. The cosmic star formation history, with its rapid rise at low z, is marginally reproduced by the local SFR history (within a factor of $\sim$2–3) if the latter is transposed to a cosmological framework and normalized to the currently observed cosmic SFR at $z = 0$. The local SFR history depends on infall, presumably in the form of infalling gas-rich satellite galaxies. These are not necessarily recognizable today if they were disrupted several Gyr ago. However, the star formation rate embodies a fossil record of such past activity. It may not be well produced by a simple exponential, or even a monotonic function, as is the common assumption in population synthesis models of the Hubble sequence. Thus, there may be a grain of truth in our naive prediction of the cosmic SFR history using the local SFR history as a template. Evidently, the normalization at $z = 0$ is highly uncertain; it is only the shape that may have significance.

4. Once we normalized the SFR history of the Milky Way to the cosmic SFR at $z = 0$, we applied our star formation model to infer the gas fraction as a function of cosmic epoch. The evolution of gas in our model matches well the observed value at low redshifts; at higher redshifts, our model requires the presence of larger gas amounts in atomic form than observed up to now. This gas is most likely in ionized form, and it may be plausibly identified with the Lyα forest gas. If this is indeed the case, then since the DLA gas fraction already accounts for the local stellar mass fraction, to within a factor of 2, any additional gas, known to be present but inferred to go into high-z star formation, must form stars that do not show up in luminous galaxies. In our model, this gas is accreted by spirals, but these spirals may be surplus to the known population.While the evidence for any excess gas at high redshift from Figure 3 is only marginal, we may speculate on its fate as follows. The resulting excess population of disk galaxies could undergo mergers that result in a population that is less visible today. One outcome might be star-forming galaxies that leave behind a substantial population of low surface brightness galaxies. Another might be merger-induced formation of a population of starburst galaxies with a truncated IMF that has no visible low-redshift relic. The early starbursting phase of such objects could play an important role in contributing to the diffuse far-infrared background light, whose measured intensity does not correspond to the aggregate diffuse flux from the precursors of any known population of galaxies.

5. The range of metal abundances observed in Lyα absorbers corresponds to the range spanned by the disk of our Galaxy during its evolution; these systems may well be (proto)galactic disks. On the other hand, the unknown amount of dust depletion makes it difficult at present to use abundance ratios as a probe of the nature of those systems. Finally, according to our simple models, D can be considerably depleted in inner disk zones, but only at low redshifts. Values observed at high redshifts (if universal) should be very close to the true primordial values.

J. S. acknowledges support from NASA, NSF, and the Blaise-Pascale chair at the Institut d'Astrophysique de Paris. We are grateful to the referee, R. Wyse, for her constructive comments, and to M. Fall for an interesting discussion.

REFERENCES

Afflerbach, A., Churchwell, E., & Werner, M. 1997, ApJ, 478, 190
Allen, C., Carigi, L., & Peimbert, M. 1998, ApJ, 494, 247
Anders, E., & Grevesse, N. 1989, Geochim. Cosmochim. Acta, 53, 197
Bazan, G., & Mathews, G. 1990, ApJ, 354, 64
Bethe, H., & Brown, G. 1995, ApJ, 445, L129
Boissier, S., & Prantzos, N. 1998, A&A, submitted
Bouwens, R., Cayon, L., & Silk, J. 1997, ApJ, 489, L21
Briggs, F. 1997, Publ. Astron. Soc. Australia, 14, 31
Burles, S., & Tytler, D. 1998, in Primordial Nuclei and their Galactic Evolution, ed. N. Prantzos, M. Tosi, & R. von Steiger (Dordrecht: Kluwer), 65
Cappellaro, E., Turatto, M., Tsvetkov, D., Bartunov, O. Pollas, C., Evans, R., & Hamuy, M. 1997, A&A, 322, 431
Cardelli, J., & Federman, S. 1997, in Nuclei in the Cosmos IV, ed. J. Gorres et al. (Amsterdam: Elsevier), 31
Carigi, L. 1996, Rev. Mexicana Astron., 4, 123
Chamcham, C., & Tayler, R. 1994, MNRAS, 266, 282
Charbonnel, C. 1998, in ASP Conf. Ser., Abundance Gradients as a Diagnostic Tool for Galaxy Evolution, ed. D. Friedli et al. (San Francisco: ASP), in press
Chengalur, J., Braun, R., & Burton, W. 1997, A&A, 318, L15
Chiapini, C., Matteucci, F., & Gratton, R. 1997, ApJ, 477, 765
Clarke, C. 1989, MNRAS, 238, 283
Clayton, D. 1997, ApJ, 484, L67
Cunha, K., & Lambert, D. 1994, ApJ, 426, 170
Dame, T. 1993, in Back to the Galaxy, ed. S. Holt & F. Verter (New York: AIP), 267
Dopita, M., & Ryder, S. 1994, ApJ, 430, 163
Edvardsson, B., Anderssen, J., Gustafsson, B., Lambert, D., Nissen, P., & Tomkin, J. 1993, A&A, 275, 101
Ferrini, F., Molla, A., & Diaz, A. 1997, ApJ, 487, L29
Ferrini, F., Molla, A., Pardi, M., & Diaz, A. 1994, ApJ, 427, 745
Fich, M., & Silkey, M. 1991, ApJ, 366, 107
Fritze-von Alvesleben, U. 1997, in IAU Symp. 187, Cosmic Chemical Evolution, ed. J. Truran & K. Nomoto (Dordrecht: Kluwer), in press
Gallego, J., Zamorano, J., Aragon-Salamanca, A., & Rego, M. 1995, ApJ, 455, L1
Geiss, J., & Gloeckler, G. 1998, in Primordial Nuclei and their Galactic Evolution, ed. N. Prantzos, M. Tosi, & R. von Steiger (Dordrecht: Kluwer), 251
Gould, A., Bahcall, J., & Flynn, C. 1997, ApJ, 482, 913
Guideroni, B., Hioon, E., Bouchet, F., & Maffei, B. 1998, MNRAS, 295, 877
Hogan, G. 1998, in Primordial Nuclei and their Galactic Evolution, ed. N. Prantzos, M. Tosi, & R. von Steiger (Dordrecht: Kluwer), 127
Iben, I., & Tutukov, A. 1984, ApJ, 284, 719
Kennicutt, R. 1989, ApJ, 344, 685
Kroupa, P., Tout, C., & Gilmore, G. 1993, MNRAS, 262, 545
Kulkarni, V., Fall, M., & Truran, K. 1997, ApJ, 484, L7
Lacey, C., Baugh, C., Cole, C., & Frenk, C. 1997, in Structure and Evolution of the IGM from QSO Absorption Line Systems, eds. P. Petitjean & S. Charlot (Gif sur Yvette: Editions Frontières), in press
Lacey, C., & Fall, M. 1986, ApJ, 290, 154
Larson, R. 1976, MNRAS, 176, 31
Linsky, D. 1998, in Primordial Nuclei and their Galactic Evolution, ed. N. Prantzos, M. Tosi, & R. von Steiger (Dordrecht: Kluwer), 283
Lu, L., Sargent, W., Barlow, T., Churchill, C., & Vogt, S. 1996, ApJS, 107, 475
Madau, P. 1997, preprint astro-ph/9709147
———. 1998, preprint astro-ph/9801005
Madau, P., Pozzetti, L., & Dickinson, M. 1997, preprint astro-ph/9708220
Malaney, R., & Chaboyer, B. 1996, ApJ, 462, 57
Marigo, P., Bressan, A., & Chiosi, C. 1996, A&A, 313, 545
Matteucci, F., & Brocato, E. 1990, ApJ, 365, 539
Matteucci, F., & François, P. 1989, MNRAS, 239, 885
Matteucci, F., & Greggio, L. 1986, A&A, 154, 279
Mayor, M., & Vigroux, L. 1981, A&A, 98, 1
McWilliam, A., & Rich, M. 1994, ApJS, 91, 749
Natarajan, P., & Pettini, M. 1997, MNRAS, 291, L28
Ng, Y., & Bertelli, G. 1998, A&A, 328, 943
Nomoto, K., Iwamoto, K., & Kishimoto, N. 1997, Science, 276, 1378
Pagel, B. 1997, Nucleosynthesis and Galactic Chemical Evolution (Cambridge: Cambridge Univ. Press)
Pain, R., et al. 1996, ApJ, 473, 356
Pei, Y., & Fall, M. 1995, ApJ, 454, 69
Pettini, M., Smith, L., King, D., & Hunstead, R. 1997, ApJ, 486, 665
Pilyugin, L., & Edmunds, M. 1996, A&A, 313, 792
Prantzos, N. 1994, A&A, 284, 477
———. 1996, A&A, 310, 106
———. 1998a, in Primordial Nuclei and their Galactic Evolution, ed. N. Prantzos, M. Tosi, & R. von Steiger (Dordrecht: Kluwer), 225
———. 1998b, in ASP Conf. Ser., Abundance Gradients as a Diagnostic Tool for Galaxy Evolution, ed. D. Friedli et al. (San Francisco: ASP), in press
Prantzos, N., & Aubert, O. 1995, A&A, 302, 69 (PA95)
Rana, N. 1991, ARA&A, 29, 129
Renzini, A., & Voli, A. 1981, A&A, 94, 175
Rocha-Pinto, H., & Maciel, W. 1996, MNRAS, 279, 447
———. 1997, MNRAS, 325, 523
Ruiz-Lapuente, P., & Canal, R. 1998, preprint astro-ph/9801141
Sackett, P. D. 1997, ApJ, 483, 103
Sadat, R., Blanchard, A., Guiderdoni, B., & Silk, J. 1997, preprint astro-ph/9712065
Samland, M., Hensler, G., & Theis, Ch. 1997, ApJ, 476, 544
Savage, B., & Sembach, K. 1996, ARA&A, 34, 279
Schaller, G., Schaerer, D., Maeder, A., & Meynet, G. 1992, A&AS, 96, 269
Shaver, P., McGee, R., Newton, L., Danks, A., & Pottasch, S. 1983, MNRAS, 204, 53
Silk, J. 1997, ApJ, 481, 703
Smartt, S., & Rolleston, W. 1997, ApJ, 481, L47
Steinmetz, M., & Muller, E. 1954, MNRAS, 276, 549
Storrie-Lombardi, L., McMahon, R., & Irwin, M. 1996, MNRAS, 283, L79
Talbot, R., Jr., & Arnett, D. 1975, ApJ, 197, 551
Tammann, G., Loefler, W., & Schroder, A. 1994, ApJS, 92, 487
Thielemann, K.-F., Nomoto, K., & Hashimoto, M. 1996, ApJ, 460, 408
Thielemann, K.-F., Nomoto, K., & Yokoi, K. 1986, A&A, 158, 17
Timmes, F., Lauroesch, J., & Truran, J. 1995a, ApJ, 451, 468
Timmes, F., Woosley, S., & Weaver, T. 1995b, ApJS, 98, 617
———. 1996, ApJ, 457, 834
Tinsley, B. 1980, Fundam. Cosmic Phys., 5, 287
Tosi, M. 1988, A&A, 197, 33
———. 1998, in Primordial Nuclei and their Galactic Evolution, ed. N. Prantzos, M. Tosi, & R. von Steiger (Dordrecht: Kluwer), 207
van den Hoek, L., & de Jong, T. 1997, A&A, 318, 231
Vilchez, J., & Esteban, C. 1996, MNRAS, 280, 720
Vladilo, G. 1998, ApJ, 493, 583
Wang, B., & Silk, J. 1994, ApJ, 427, 759
Wielen, R., Fuchs, B., & Dettbarn, C. 1996, A&A, 314, 438
Woosley, S., & Weaver, T. 1995, ApJS, 101, 181 (WW95)
Wyse, R., & Gilmore, G. 1995, AJ, 110, 2771
Wyse, R., & Silk, J. 1989, ApJ, 339, 700